# Supporting Information:

# Plasmon-Mediated Chemical Surface Functionalization at the Nanoscale

Mai Nguyen[a,b], Aazdine Lamouri[a], Chrystelle Salameh[a], Georges Lévi[a], Johan Grand[a], Leïla Boubekeur-Lecaque[a], Claire Mangeney[a*], and Nordin Félidj[a†]

*(a) Interfaces, Traitements, Organisation et Dynamique des Systèmes, Université Paris Diderot, Sorbonne Paris Cité, CNRS UMR 7086, 15 rue Jean-Antoine de Baïf, 75205 Paris Cedex 13, France and*

*(b) USTH, University of Science and Technology of Hanoi, 18 Hoang Quoc Viet, Hanoi, Vietnam*

[*] corresponding author: mangeney@univ-paris-diderot.fr

[†] corresponding author: nordin.felidj@univ-paris-diderot.fr

**Computational section**

All calculations were carried out using the Gaussian 09 suite of programs[1] using the B3LYP exchange and correlation functional[2] along with the 6-311++G(d,p) basis set for all atoms but gold.[3] The LANL2DZ basis set consisting of Effective Core Potential (ECP) and double-$\xi$ quality functions for valence electrons was employed for Au.[4] The structures were optimized without symmetry constraint. The vibrational frequencies and normal modes were calculated within the harmonic approximation and a scaling factor of 0.976 was chosen on the basis of previously published work.[5]

*Simulated Raman spectra*

The grafting of HEBDT diazonium salt on gold nanostripe surface was modeled by a hybrid system based on the pyramidal gold cluster $Au_{20}$. The spontaneous dediazonation of HEBDT on gold surface leads to monolayer or multilayers represented by the MeB-$Au_{20}$ and MeBiPh-$Au_{20}$ adducts respectively (see Figure SI2a). DFT calculations were conducted on model system featuring 4-methylphenyl bonded to the vertex of pyramidal gold cluster $Au_{20}$ through Au-C bond. Figure SI2a shows the experimental SERS spectrum for HEBDT on gold nanostripes and the calculated Raman spectra for the two envisaged adducts on gold surface. Despite the simplicity of the model, a good agreement is found between the experimental SERS spectra and the simulated Raman spectra by DFT for the multilayer model MeBiPh-$Au_{20}$. More precisely, the observed band at 1626 $cm^{-1}$ is only reproduced by MeBiPh-$Au_{20}$ model (band predicted at 1620 $cm^{-1}$).

---

[1] R. A. Gaussian 09, Frisch, M. J.; Trucks, G. W.; Schlegel, H. B.; Scuseria, G. E.; Robb, M. A.; Cheeseman, J. R.; Scalmani, G.; Barone, V.; Mennucci, B.; Petersson, G. A.; Nakatsuji, H.; Caricato, M.; Li, X.; Hratchian, H. P.; Izmaylov, A. F.; Bloino, J.; Zheng, G.; Sonnenberg, J. L.; Hada, M.; Ehara, M.; Toyota, K.; Fukuda, R.; Hasegawa, J.; Ishida, M.; Nakajima, T.; Honda, Y.; Kitao, O.; Nakai, H.; Vreven, T.; Montgomery, Jr., J. A.; Peralta, J. E.; Ogliaro, F.; Bearpark, M.; Heyd, J. J.; Brothers, E.; Kudin, K. N.; Staroverov, V. N.; Kobayashi, R.; Normand, J.; Raghavachari, K.; Rendell, A.; Burant, J. C.; Iyengar, S. S.; Tomasi, J.; Cossi, M.; Rega, N.; Millam, J. M.; Klene, M.; Knox, J. E.; Cross, J. B.; Bakken, V.; Adamo, C.; Jaramillo, J.; Gomperts, R.; Stratmann, R. E.; Yazyev, O.; Austin, A. J.; Cammi, R.; Pomelli,

C.; Ochterski, J. W.; Martin, R. L.; Morokuma, K.; Zakrzewski, V. G.; Voth, G. A.; Salvador, P.; Dannenberg, J. J.; Dapprich, S.; Daniels, A. D.; Farkas, Ö.; Foresman, J. B.; Ortiz, J. V.; Cioslowski, J.; Fox, D. J. Gaussian, Inc., Wallingford CT, 2009.

[2] a) A. D. Becke, J. Chem. Phys.1993, 98, 5648; b) C. T. Lee, W. T. Yang, R. G. Parr, Phys. Rev. B 1988, 37, 785.

[3] a) T. Clark, J. Chandrasekhar, G. W. Spitznagel, P. V. Schleyer, J. Comput. Chem. 1983, 4, 294; b) M. M. Francl, W. J. Pietro, W. J. Hehre, J. S. Binkley, M. S. Gordon, D. J. Defrees, J. A. Pople, J. Chem. Phys. 1982, 77, 3654.

[4] P. J. Hay, W. R. Wadt, J. Chem. Phys. 1985, 82, 270.

[5] S. Z. Fairchild, C. F. Bradshaw, W. S. Su, S. K. Guharay, Applied Spectroscopy 2009, 63, 733.

[6] Mesnage, A.; Lefèvre, X.; Jégou, P.; Deniau, G.; Palacin, S. Spontaneous Grafting of Diazonium Salts: Chemical Mechanism on Metallic Surfaces, *Langmuir*, **2012**, *28*, 11767–11778.

[7] Canning, J.; McCrudden, K.; Maskill, H.; Sexton, B. Rates and mechanisms of the thermal solvolytic decomposition of arenediazonium ions, *Journal of the Chemical Society-Perkin Transactions*, **1999**, *2*, 2735–2740.

[8] Lehr, B. E. Williamson, B. S. Flavel, A. J. Downard, Reaction of Gold Substrates with Diazonium Salts in Acidic Solution at Open–Circuit Potential, *Langmuir*, **2009**, *25*, 13503-13509.

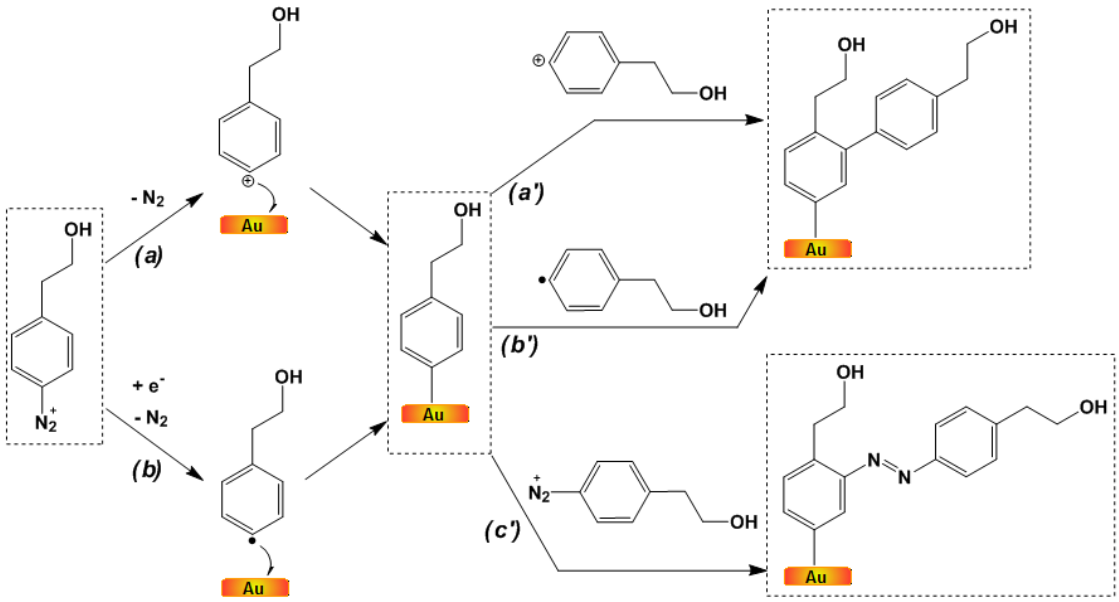


Figure 1: Proposed mechanisms, from literature, of aryl film grafting (derived from diazonium salt molecules) on a gold surface: (a) the cationic pathway was proposed in the case of the thermal decomposition of diazonium salts and was described as follows: first, the heating of diazonium salts in water was reported to lead to aryl cations. Then, due to their short lifetime in water, only those formed near the gold surface would attach to it.[6,7] The aryl cations also react on the already grafted aryl groups, leading to the formation of a polyaryl layer on the surface (route a'). (b) The radical pathway would proceed via an electron transfer from the gold to the diazonium cation, leading to its reduction and to the formation of highly reactive aryl radicals at the substrate-solution interface able to bind to the surface and to form a covalently linked aryl layer. In a following step, other aryl radicals would contribute to the growth of the films by their addition on the aromatic rings already grafted on the substrate, followed by the elimination of $H^+$ (route b').[8] The polyaryl film growing by azo coupling on the already grafted phenyl layer was also reported, as illustrated in route c'.

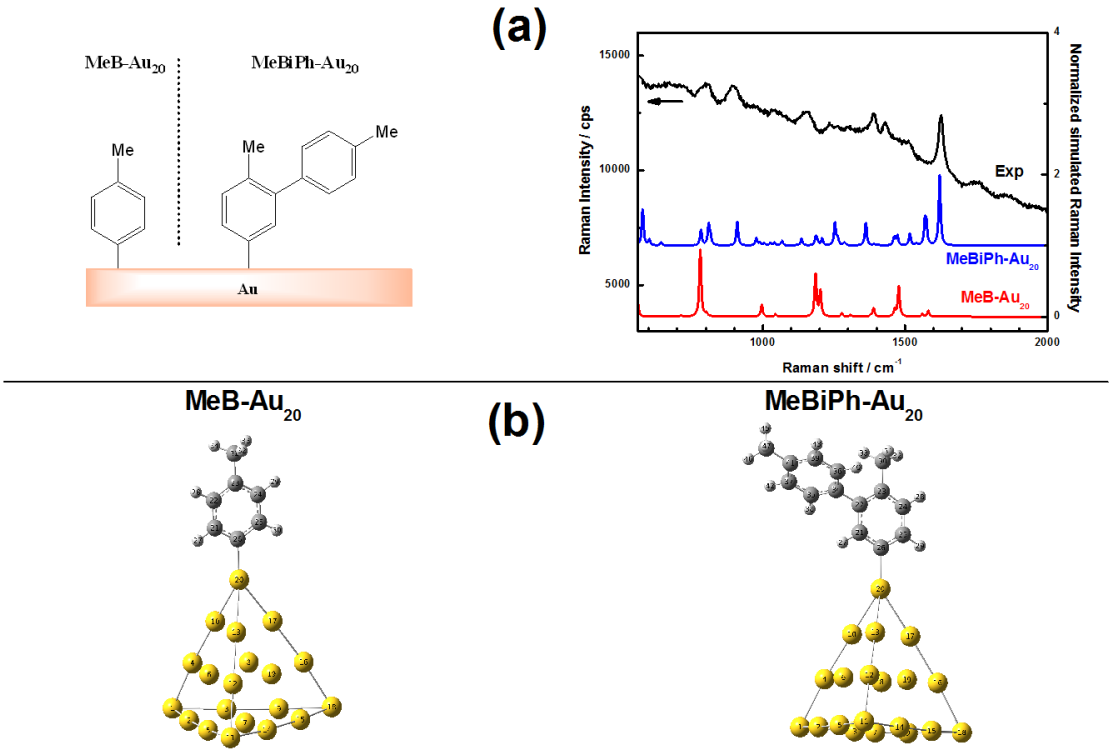


Figure 2: (a) 4-Methylphenyl adducts envisaged for DFT modelling: (black) Experimental SERS spectrum recorded on gold nanostripes ($\lambda_{exc}$=633 nm; laser power $P$=1 mW; acquisition time: 3×30 sec.). Simulated Raman spectra of 4-methylphenyl adduct on a pyramidal gold cluster Au20 as monolayer MeB-$Au_{20}$ (red), as bilayer MeBiPh-$Au_{20}$ (blue); (b) Optimized geometries for MeB-$Au_{20}$ and MeBiPh-$Au_{20}$.

**Table of cartesian coordinates MeB-$Au_{20}$**

| Tag | Symbol | X | Y | Z |
|---|---|---|---|---|
| 1 | Au | 0.0338250 | 0.0572490 | -0.0398070 |
| 2 | Au | 0.0076890 | 0.0154130 | 2.7535270 |
| 3 | Au | 2.5917240 | 0.0246550 | 1.0815630 |
| 4 | Au | 0.7704680 | 2.4992920 | 1.1238130 |
| 5 | Au | 0.1462040 | 0.0702650 | 5.4780800 |
| 6 | Au | 0.7199250 | 2.5254940 | 4.0313600 |
| 7 | Au | 2.6409360 | -0.0748660 | 3.9886760 |
| 8 | Au | 3.4486580 | 2.5366880 | 2.2548730 |
| 9 | Au | 5.0208370 | 0.0983480 | 2.3242110 |
| 10 | Au | 1.6165240 | 4.7764710 | 2.4288790 |
| 11 | Au | 0.4522270 | 0.2297580 | 8.2506130 |
| 12 | Au | 1.0614620 | 2.6179080 | 6.9174700 |
| 13 | Au | 1.7626530 | 4.8351760 | 5.4430950 |
| 14 | Au | 2.8839340 | 0.1454370 | 6.8791120 |
| 15 | Au | 5.1761330 | 0.1626000 | 5.3968560 |
| 16 | Au | 5.9329360 | 2.6506460 | 3.7650520 |
| 17 | Au | 4.2728850 | 4.8504720 | 3.7995860 |
| 18 | Au | 7.4227510 | 0.2778820 | 3.7405650 |
| 19 | Au | 3.6148030 | 2.6056510 | 5.5224810 |
| 20 | Au | 2.4822970 | 7.0879100 | 3.8586670 |
| 21 | C | 1.1789960 | 9.8078790 | 3.9452680 |
| 22 | C | 1.1371120 | 11.2030640 | 3.9800710 |
| 23 | C | 2.3093110 | 11.9649280 | 3.9853720 |
| 24 | C | 3.5329550 | 11.2886010 | 3.9483750 |
| 25 | C | 3.5897020 | 9.8945100 | 3.9133140 |
| 26 | C | 2.4089190 | 9.1524730 | 3.9121180 |
| 27 | H | 0.2498520 | 9.2500740 | 3.9407950 |
| 28 | H | 0.1727400 | 11.7018170 | 4.0017240 |
| 29 | H | 4.4595920 | 11.8549390 | 3.9446370 |
| 30 | H | 4.5555680 | 9.4039870 | 3.8837370 |
| 31 | C | 2.2579610 | 13.4723340 | 4.0554080 |
| 32 | H | 2.3354190 | 13.8193930 | 5.0916810 |
| 33 | H | 3.0807350 | 13.9258610 | 3.4974790 |
| 34 | H | 1.3199440 | 13.8582420 | 3.6501470 |

## Table of cartesian coordinates MeBPh-$Au_{20}$

| Tag | Symbol | X | Y | Z |
|---|---|---|---|---|
| 1 | Au | 0.2848340 | 0.3457320 | -0.4472100 |
| 2 | Au | 0.0521280 | 0.1542560 | 2.3304410 |
| 3 | Au | 2.7520220 | 0.2357450 | 0.8574610 |
| 4 | Au | 0.9398300 | 2.7160740 | 0.8966690 |
| 5 | Au | -0.0123970 | 0.0667330 | 5.0569370 |
| 6 | Au | 0.6747250 | 2.5895270 | 3.7895110 |
| 7 | Au | 2.5858100 | -0.0180040 | 3.7504550 |
| 8 | Au | 3.5285050 | 2.6780680 | 2.2225510 |
| 9 | Au | 5.0831210 | 0.2272450 | 2.2772360 |
| 10 | Au | 1.6886270 | 4.9138010 | 2.3785420 |
| 11 | Au | 0.0892740 | 0.0760420 | 7.8487600 |
| 12 | Au | 0.8025260 | 2.5293420 | 6.6937380 |
| 13 | Au | 1.6193540 | 4.8188330 | 5.3929680 |
| 14 | Au | 2.6158250 | 0.0487670 | 6.6587150 |
| 15 | Au | 5.0107170 | 0.1293520 | 5.3517250 |
| 16 | Au | 5.8927090 | 2.6950060 | 3.9160170 |
| 17 | Au | 4.2407640 | 4.9008140 | 3.9521190 |
| 18 | Au | 7.3740040 | 0.3167010 | 3.8734280 |
| 19 | Au | 3.4501920 | 2.5718400 | 5.4923960 |
| 20 | Au | 2.4587150 | 7.1437810 | 3.9722470 |
| 21 | C | 1.1764500 | 9.8700430 | 3.9707100 |
| 22 | C | 1.1071850 | 11.2737560 | 3.9852450 |
| 23 | C | 2.3010800 | 12.0242610 | 3.9990820 |
| 24 | C | 3.5189980 | 11.3369190 | 4.0074350 |
| 25 | C | 3.5843970 | 9.9441680 | 4.0007680 |
| 26 | C | 2.4014550 | 9.2099540 | 3.9819890 |
| 27 | H | 0.2479340 | 9.3113770 | 3.9673130 |
| 28 | H | 4.4443260 | 11.9051850 | 4.0038880 |
| 29 | H | 4.5510410 | 9.4548090 | 4.0019170 |
| 30 | C | 2.3054870 | 13.5358610 | 3.9758690 |
| 31 | H | 2.1399280 | 13.9575080 | 4.9724700 |
| 32 | H | 3.2678310 | 13.9098290 | 3.6201470 |
| 33 | H | 1.5213460 | 13.9313590 | 3.3272930 |
| 34 | C | -0.2407580 | 11.9123580 | 3.9702980 |
| 35 | C | -1.1341940 | 11.6625130 | 2.9218710 |
| 36 | C | -0.6728560 | 12.7412240 | 5.0142160 |
| 37 | C | -2.4069850 | 12.2294290 | 2.9127070 |
| 38 | H | -0.8251910 | 11.0237090 | 2.1015250 |
| 39 | C | -1.9464710 | 13.3012410 | 5.0037760 |
| 40 | H | -0.0138020 | 12.9314510 | 5.8539670 |
| 41 | C | -2.8366070 | 13.0608810 | 3.9506240 |
| 42 | H | -3.0761130 | 12.0199670 | 2.0840200 |
| 43 | H | -2.2574840 | 13.9294310 | 5.8329350 |
| 44 | C | -4.2060060 | 13.6956160 | 3.9305640 |
| 45 | H | -4.1538770 | 14.7331170 | 3.5825300 |
| 46 | H | -4.8837300 | 13.1590960 | 3.2630220 |
| 47 | H | -4.6535190 | 13.7097420 | 4.9277460 |

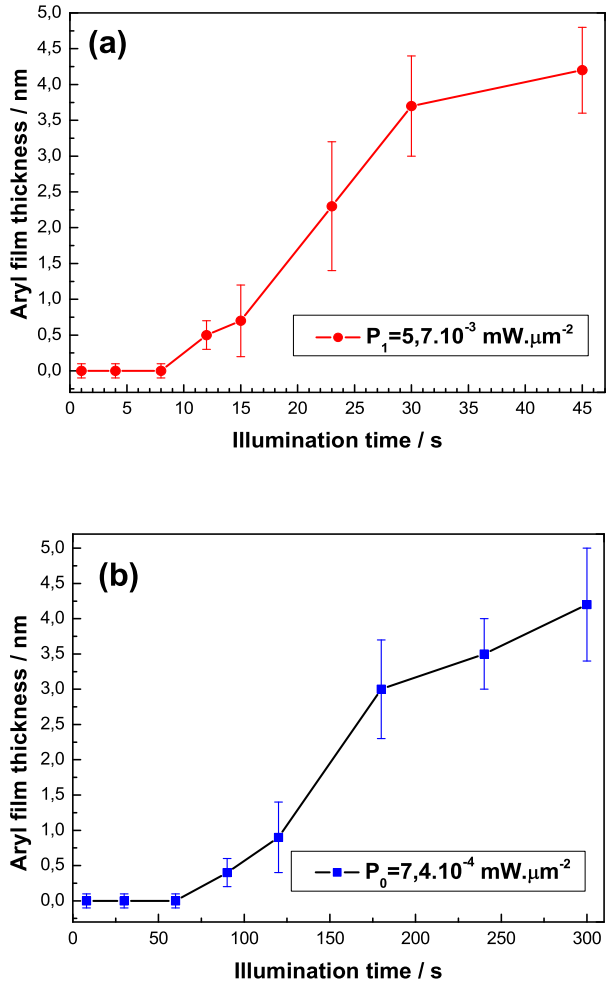


Figure 3: Aryl film thickness deduced from AFM measurements, versus the illumination time, for two different laser powers: $P_1$=0.86 mW.$\mu$m$^{-2}$ (a) and $P_0$=0.089 mW.$\mu$m$^{-2}$ (b) respectively. The gold nanostripes were homogeneously immersed in a solution of HEBDT (concentration 3x10$^{-3}$M). The optical exposure was performed under normal incidence, and the He-Ne laser ($\lambda_{inc}$ = 633 nm) was focused on the stripe array through a microscope objective ($\times$ 100, numerical aperture N.A.#0.8), resulting in a circular laser spot of $\sim$3 $\mu$m diameter at the surface.

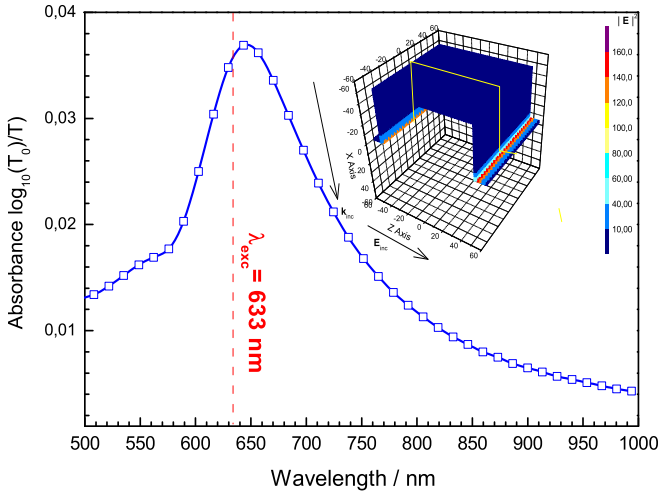


Figure 4: Calculated absorbance by the DDA method for a gold stripe target with a width of W = 125 nm and height of H = 50 nm. The incident polarization was set perpendicular to the stripe. Inset: 3D mapping of the near-field enhancement on a unit cell length of W = 125 nm wide stripe, and height H = 50 nm.

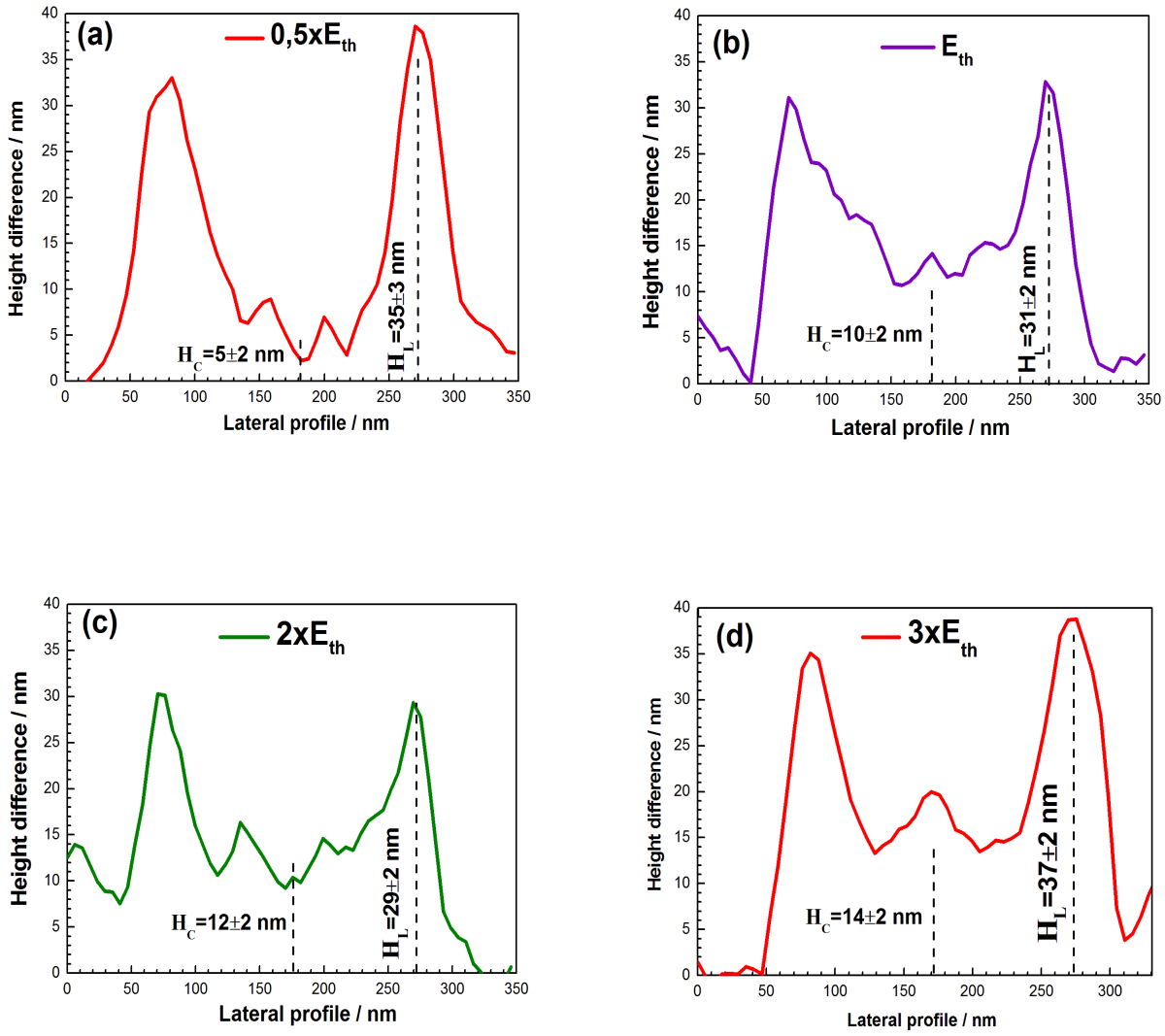


Figure 5: Differential lateral profiles of a single gold nanostripe, by subtracting the topographical profiles of the cross sections of the gold stripe, before and after illumination in transverse polarization. The differential profiles are displayed for the following energy dose: (a) $0.5\times E_{th}$, (b) $E_{th}$, (c) $2\times E_{th}$, and (d) $3\times E_{th}$, with $E_{th}$=5.5 mJ.$\mu$m$^{-2}$. $H_C$ indicates the height of the aryl film in the center of the stripe, while $H_L$ indicates the height of the aryl film at the location of the lobes.

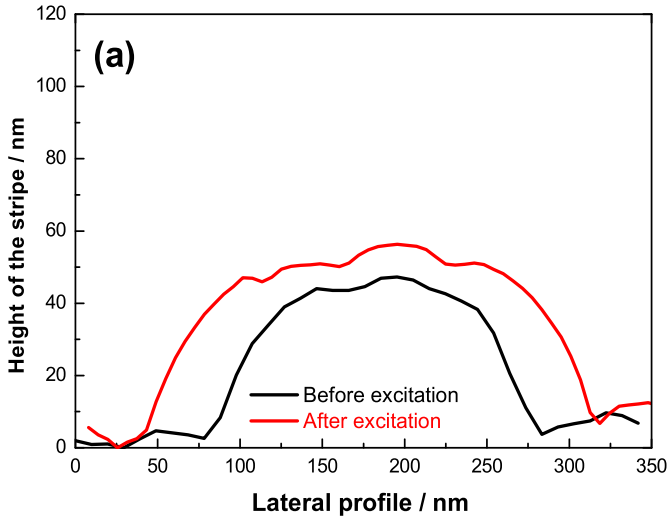


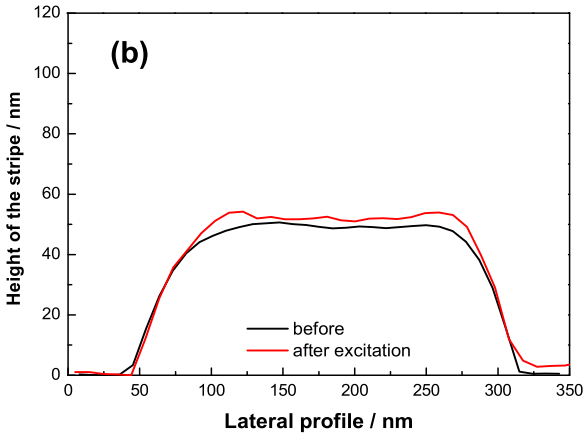


Figure 6: For an energy dose E=3x$E_{th}$: (a) profile of the lateral cross section of a single stripe before and after illumination in transverse polarization (under LSP excitation). The aryl film thickness in the center of the stripe is $H^C_{aryl} \sim 14$ nm; (b) profile of the lateral cross section of a single stripe before and after illumination in longitudinal polarization (no LSP excitation). $H^C_{aryl}$ is only $\sim 4$ nm in the center of the stripe.